Improving the conductivity and flexibility of chips fabricated from a copolymer PDMS-PEI and graphene assembled with nano metals

Ameen Abdelrahman (abda02@uqat.ca)
UQAT: Universite du Quebec en Abitibi Temiscamingue https://orcid.org/0000-0002-7177-2687
Fouad Erchiqui
UQAT: Universite du Quebec en Abitibi Temiscamingue
Mourad Nedil
UQAT: Universite du Quebec en Abitibi Temiscamingue

Research Article

Keywords: copolymers, impedance, assembled metals, graphene, self-healing

Posted Date: February 24th, 2021

DOI: https://doi.org/10.21203/rs.3.rs-232116/v1

Abstract

Our work aims to make a unique polymer to be used as a conductive and flexible chip antenna. Its properties are robustness, rigidity, stretchability, and good conduction. The fabricated composite is composed of two copolymers, PDMS and PEI, assembled with nano metals (Cu, Ag), and graphene nanoparticles as a matrix. Nano metals fill out the inter-layer space, and polymer voids reinforce the crosslinker. Graphene/metal nanoparticles help make chelating complexes using metallic bonds, enhancing the polymer's conductivity from 1.87* 10^{-4} to 5.64*10^{-6} σ Scm^{-1}. We analyze the conductivity, self-healing, and surface morphology of fabricated composite using different spectroscopic techniques, such as electrochemical impedance (EIS), SEM, TEM, IR, UV, and a particle size analyzer.

1. Introduction

Flexible (stretchable) electronics fabricated with electronic innovation technology incorporates an organic/inorganic conductive component with nonconductive polymers or metal deposits substrates. Stretchable electronics have gotten much attention due to their unique properties like efficiency, flexibility/ductility, low-cost cook-up processes, and broader application potential in displays, biosensors, RFID, wearable antenna tags, and devices [1]. One important value of stretchable electronics is that materials keep conductivity under great strain during mechanical movement. The highly diverse properties of polymeric materials such as healing, flexibility, robustness, and conductivity are the main reasons they are applicable in different fields. They are particularly useful when integrated or impregnated with different materials, like silver nanowire (AgNW) [2, 3], carbon nanotubes (CNT) [4, 5], graphene (GR) [6–9], polyaniline (PANI)(10), or polypyrrole (PPY) [11, 12].

Poly(dimethylsiloxane) (PDMS) is one of the most likely di-electric materials used to fabricate microfluidic electronic devices. The material's cost, simple fabrication process, rapid prototyping, excellent optical transparency, and gas permeability have been widely publicized. Although PDMS has many advantages, its high hydrophobicity (water contact angle ∼108° ± 7°) usually limits its applications. Recently, copolymers have been getting more attention due to their applications in aerospace, microelectronics, printed circuits, adhesives, thermoplastic elastomers, and organophilic pervaporation [13–16]. Furthermore, the high demand for microelectronics and nanoelectronic devices increases because they are highly-precious and used to control dimensional structures in wafer-scale manufacturing [17–20]. The device invention methodologies are already well known in electronic manufacture using silicon chips miniaturization on a large scale [21–22].

On the other hand, alternative methodology builds on approaches to block copolymer (BCP) as self-assembly nanostructure creation is increasingly and rapidly approached by researchers [23]. Approaches can create sub-10 nm structures with low costs [24, 25]. BCPs like polyethyleneimine -b-polymethylmethacrylate (PEI-b-PMMA), polylactic acid-b-polystyrene (PLA-b-PS), polystyrene-b-polydimethylsiloxane(PS-b-PDMS), and polyethylene oxide-b-polystyrene (PEO-b-PS) of cylindrical, lamellar, or spherical structure joints in different strategies to modify or control the substrate and

alignment pattern have been used to pioneer nano lithographic disassembly [26, 27]. However, conventional conductors are not stretchable, while traditional elastomers like polystyrene, natural rubber (NR), and poly(dimethylsiloxane) (PDMS) are not conducive. Two methods have been used to achieve stretchable interconnected interlink filler. The first involves making wavy or mesh configurations by adding conductive materials, materials with tensile strain, and elastic materials [28]. The second method involves filling the gaps or interspace of polymers with conducting material [29, 30].

Copolymerization is one of the best ways to prepare new polymeric materials. By combining two structures, its specific properties have different chemical or physical properties as one block polymer chain. It has been established that the integration between polysiloxane and polyimide improves efficiency and polyimide's processability and its mechanics augment polysiloxane's properties. The other beneficial properties of poly(imide siloxane) copolymers should be considered, high hydrophobicity, oxidizing resistance to other oxidizing agents and environment, and adhesion di-electric constants, high flexibility, and robustness [31–37]. Moreover, the stability (thermoplastics to thermoplastic elastomers) of poly(imide siloxane) copolymers, which based on composition and structure[38, 39]. Therefore, the copolymers have become highly sought after for many application such as microelectronic, adhesives, biosensors, communication, and aerospace applications [31, 35, 39].

PDMS is characterized by a low glass transition temperature of − 127ºC, in addition to the shear elastic modulus 250 kPa, while a specific gravity range between 0.91 to 1.00 with a molecular weight of 10–60 × 10^3 gmol − 1. PDMS is an inert polymer and hydrophobic chemical environment partially dissolved in solvents such as pentane, xylene, and trimethylamine [40]. Studies show that carbon nanotubes (CNTs) have an electrical conductivity of 10^4–10^5 S cm-1, high carrier mobility of 1000–4000cm2 V^{-1} s^{-1}, thermal stability up to 700^0C in air Young's models of between 0.27–1.25 TPa, and thermal conductivity of 3000–6600 W m-1 K-1 [41–43]. The electrically conductive CNT/polymer composites have potential applications, especially in electromagnetic shielding,[44, 45] energy harvesting, biomedical devices., supercapacitors, [46, 47] sensors, [48, 49] and smart actuators [50, 51]. Since CNT/polymer composites are mechanically resilient, cost-effective, lightweight, easily process able, scalable, and compliant, they can be used in electric heating elements [16–18]. Polydimethylsiloxane (PDMS), a type of silicon-based elastomer, has excellent properties, including optical transparency, chemical/biological extinction, flexibility, nontoxicity, and gas permeability [53, 54]. PEI (polyethyleneimine) is applicable in different industries. Its various properties, like water base polymer selectivity (it dissolves in hot water), give it good chemical and thermal stability and mechanical properties [55]. Different studies have been done on the assembly of a PEI/metal complex. For instance, Kurdi and Tremblayas' work on hollow fiber membranes used O_2/N_2 adsorption on the surfaces [56]. Ren et al. have also studied the effect of different solvents on PEI's morphology [57].

Many studies have investigated filling voids detected by SEM using three different thermal degradations of copolymers at different scanning calorimetry (DSC) measurements, with semi-crystalline polymers or polymer/filler interactions. These studies find that its mechanical properties (neat matrices and in PNCs) increase the degree of crystallinity-related impact [58–64]. In other words, many studies worked on the

association between the application of a graphene matrix [67–71] with polydimethylsiloxane (PDMS)/graphene and the degree of crystallinity. This was given more attention by a polymer scientists who demonstrated the new composite's mechanical, electrical, and thermal properties [70–73]. For example, a PDMS/CNTs or graphene matrix has many applications, especially in the electronic and biomedical fields [74, 75]. The PDMS/graphene interaction or interfaces were illustrated by the p-a bond between the carbon of one methyl group of the polymer and the p-electron-cloud on the nanotubes' surface. The interaction of CH-p causes the inter-intermolecular forces [76]. The electrolyte polymer has good ionic conduction, and its prevalent charge carriers are ions. Thus electrolytes are also electronically conductive. An electrolyte can exist in a liquid, solid, and quasi-solid, or gel form. The aqueous KCl solution is an excellent liquid electrolyte [77], and α-Ag I is a solid electrolyte conductor [80]. Polymer conductivity is achieved by ionic salts or nano metallic particles assembled or dissolved in polymers to be electrolytes. For example, LiClO4 suspended in polyethylene oxide (PEO) solution is a polymer electrolyte [78]. The resistance of an alternating current (ac) transition in the substance is measured by electrical impedance, which Oliver Heaviside introduced in the 1880s with his work on electrical circuits [79]. Electrochemical impedance spectroscopy (EIS) is one of the electrochemistry techniques used to measure polymer conductivity. It uses three electrodes (count, reference, and stander electrode). EIS can detect resistance (ohms) by the applied potential to determine the conductive polymer's electric properties on the applied Frequency-dependent impedance spectrum. Many studies had been done on the presence of polymer electrolytes [81–86].

This paper aims to describe the fabrication of a flexible conductor copolymer composed of polyethyleneimine and polydimethylsiloxane assembled in a thin layer of graphene and nanoparticulate metals made from silver and copper. Various characterizations have been conducted on copolymers to evaluate which composite can produce a flexible, stretchable antenna in future work.

2. Materials And Methods

2.1. Materials

Graphene nanopowders (purity > 99%, 300 mesh) were supplied by Sigma-Aldrich Co., Ltd. (Canada). Most of the chemicals used were copper sulfates and silver nitrates. Polyethyleneimine (PEI), n-Hexane, and THF were purchased from Sigma Aldrich, Canada. Polydimethylsiloxane (PDMS) was purchased from Sylgard R 184, Dow Corning Corporation, Canada.

2.2 Methods

2.2.1 Assembly of nanographene on PDMS

PDMS dispersion (3 mg/mL, 2 mL), THF, and graphene (6 mg) was added to a 100 ml glass beaker and mixed until homogenous using an XHF-DY homogenizer at 3500 rpm for 15 minutes. The colloidal solution was then further mixed using ultrasonication with adjustable t temperature at 45°C for one hour.

2.2.2 Preparation of the PEI composites matrix

We took 3ml of 0.2 M electrolyte solution, $CuSO_4$, and $AgNO_3$, and heated it until 40°C. Then we added PEI (dissolved in hot water), after that stirring for 5 hours. Ultrasonication was used until homogeneous, and the complete dispersal of NPs inside polymers chains occurred.

2.2.3 Copolymers (PEI –g-PDMS) molding

A percent (50/50v:v) of PDMS/graphene and composites was mixed in a PEI solution, then curing agent B was added in a weight ratio of 10:1. The mixture was put under a vacuum oven at room temperature for 30 minutes to remove the bubbles completely, and then it was picked at 60°C for four hours.

Afterward, from our understanding, carbon nanomaterials have good electric properties because charged electrons move easily through carbon by forming resonance outside of the bonds (C = C) that transfer the electrical charge p high to permit electrical conductivity. Subsequently, adding or grafting a small number of carbon nanoparticles or graphene alternatives to nonconductive polymers will improve the impact of their surface, increase surface area, and reduce resistivity. For that reason, polymer nanocomposites could be applied to biological sensors, electronic fabrication, or automotive and aerospace manufacturing. Extensive research on assembling or grafting different sorts of polymers by different composites ceramic or inorganic materials to improve the different characteristics of new composites (mechanicals, chemicals, and thermal) has been carried out. One factor should be considered: the preparation method and the process of creating the nanocomposite matrix, and physical properties like the aggregation and deposition or depletion of carbon sheets can affect its electrical performance. Nanofibers, graphene sheets, and nanotubes (SWNT or MWNT) produced by different methods, the adhesion technique, matrix alignment, the dispersion between the nanomaterial and polymer, even chemical modification and purification have a great impact on the electrical conductivity of nanocomposites.

The imaginary peak is a part of the electric modulus (M") supply input on long-domain of dipole motion, which results from the imaginary part of the impedance spectrum (Z") (imaginary for the copolymer under discussion). The copolymer PDMS-g-PEI behaves like an electrolyte solution of different specious with dipole sites. On the other hand, there are interfaces between the nanoparticle dipoles and pairing electron on N atoms in PEI, which results in circles of resonance inside graphene structure, as shown in Fig. 1.

3. Results And Discussion

3.1 Characterization

FTIR spectra were acquired using a Nicolet iS50 IR spectrometer association with KBr pellets. The PDMS morphology of graphene, PEI -NPs, and copolymer were investigated using a transmission electron

microscope (JEM-2100F, Japan). The Current (I)–voltage (V) curves were measured by using an electrochemical working station (AUTO LAB PGSTAT100).

EIS characterization

The detection impedance of composite materials used for electrodes EIS analysis or electrochemical analysis was investigated using a Multidetector connected with a Frequency Analyzer (MPFA). Its potentiostat-galvanostat joint with eight channels is used for electrochemical characterization and electrolytes battery studies (10V, 4A). It is designed as Corrware/Corrview system to facilitate the implementation of all electrochemical methods associated with the 1255B frequency analyzer to detect or estimate OCV and CVT. This is achieved by taking a thin layer or cylinder from different electrolyte polymers, then putting them in a sample shape (e.g., coin cell) sandwiched between two proper electrodes conducted through impedance at frequencies between 2MHz and 1.5 kHz at open cycle voltage (OCV = 0.39) using three electrodes, a working electrode (glass), a reference Ag/AgCl electrode and a counter electrode.

Real impedance (Z') indicated the sample's ohmic resistance, while imaginary (Z") calculates non-ohmic resistance. We can summarize the EIS characterization by some inhomogeneous changes regarding the polymer conductivity. The analysis mechanism is related to any development or change of double-layer electrode, and polymer surface is visible as a minimum of Z" as a frequency function. A Nyquist plot curve applicable to electronic circuits is used to estimate the electrical or electrochemical parameters, especially on charge transfer and resistance in the system. See Fig. 2 below.

We noticed an inverse proportion of resistance conductivity by investigating the specific resistance of different prepared compounds (PDMS-g-PEI, electrolyte Ns, PDMS–graphene, and PEI –NPS), which depends on the free of movement of ionic charges inside the compound. In the case of the liquid electrolyte (0.2M of CuSO4 and AgNO3), we found a lower resistance (Z' value) compared to another flexible, stretchable polymer. We also recorded that the conductivity of PEI/NPS is higher than PDMS-graphene. It might be that the NPS (Ag, Cu) created new sites with an amines group (dual characterization). A pair of electrons charge the transfer, and an Ag-Ag and Cu-cu metallic bond losses an electron, and numerous electron charges feed the polymers.

On the other hand, we found that the PDMS-graphene conductivity is increased by coupling or co blocking with PEI/NPS. Our explanation for that phenomena could be that free ions created by PEI/NPs cause a resonance(π-π) bond inside the grapheme structure (PDMS-graphene). Otherwise, due to nanoparticles (Ag and Copper) impregnated inside a matrix synthesis, different active sites are needed to improve charge or ions. Table 1 shows the calculation for the electric conductivity using the following expression,

$$R = \rho\frac{L}{A} \quad \text{and} \quad \sigma = \frac{1}{\rho} = \frac{L/A}{R}$$

where ρ indicates the material resistivity, L is the material's length, A is the polymer area, and L/A is the cell constant. Since R can be acquired by the EIS plot, we can detect the σ for prepared composites polymer. The conductivity of the electrolyte solution PDMS-b-PEI-PEI-NPs-PDMS-Graphene is shown below in Table 1.

Table 1 shows the conductivity measurements of prepared materials.

Materials composites	L/A (cm^{-1})	$R_b A$ (Ω cm^2)	σ (Scm^{-1})
PDMS-b-PEI	$3.3x10^{-2}$	$6.09 x10^{2}$	$1.87x10^{-4}$
PDMS-Graphene	$2.56x10^{-2}$	$3.55x10^{3}$	$1.04x 10^{-5}$
PEI-NPs	$1.4x10^{-7}$	$4.55x10^{4}$	$3.67x10^{-7}$
Electrolyte solutions	—	—	$5.64 x10^{-6}$

Fourier transform infrared spectroscopy.

FTIR analysis was carried out on 50μm thick PDMS-b-PEI, PEI-NPs, and PDMS-Graphene film, to investigate the effect of grafting and assembled of composites on the properties of functional groups of polymers. The FTIR characterization was done by an Equinox 55 FTIR Spectrometer (Billerica, MA, Bruker Optics) provided a KBr beam splitter. Each prepared sample has been scanned at ambient temperature with a resolution of 4 cm − 1 under inert nitrogen flux flow to eliminate any water vapor. The data were recorded in the wavelength around 4000–400 cm − 1 using Bruker Optics OPUS (Bruker Optics) 4.0 software.

IR characterization

Figure 3 shows a comparison between different composites of PDMS/graphene. In the FTIR spectra, we found two spectra at 845 and 1585 cm-1 for the carbon structure of carbon in graphene, which correspond to v(C = O) and corresponds to peak 1743 cm-1 at typical of carboxyl moieties. Another carboxyl group slightly appears around t0 1346 cm-1. A weak peak noticed at 1575 cm-1, appoint to -C = C in the spectrum might be resonance phenomena inside the graphene ring related to electron transfer or bi -bi bond interface interaction between graphene structure and SiO3 of PDMS polymer at band 785 cm-1 and 915 spectra provides good evidence for v(Si-OH) and δ(OH) respectable out of the plane. Also, at 1105 cm-1 is concerned with Si-O-Si and Si-O-C vibrations. There is a high-intensity absorbency at 1740 cm-1, a spectrum corresponding to the v(C = O) group vibration, which is shifted by a combination of organic carbon chain graphene. The explanation for the spectrum of PDMS/graphene detection signals is that it is assigned at 1257 cm-1 and 1099 cm-1 inclusive Si-C stretching vibration. The other reason for forming the matrix polymer or composites matrix is that no spectra appear. Functionalized graphene is not found between 790 and 950 cm-1, which means coordination of the bond related to Si-OH groups.

Figure 3 shows a comparison between different composites PDMS/graphene FTIR spectra. We found two spectra at 845 and 1585 cm-^{1} for the carbon structure of carbon in graphene, according to Kastnert (1994) and Saito (1998). These correspond to v(C = O) and a peak of 1743 cm^{-1} at typical carboxyl moieties. Another carboxyl group makes a slight appearance around t0 1346 cm-1. A weak peak was noticed at 1575 cm-1, appoint to -C = C in the spectrum. It might be resonance phenomena inside graphene ring related to electron transfer or bi -bi bond interface interaction between graphene structure and SiO3 of PDMS polymer at band 785 cm-1 and 915 spectrum—this is great evidence that v(Si-OH) and v (OH) is respectable out of the plane. Also, at 1105 cm-1 is concerned for Si-O-Si and Si-O-C vibrations. High-intensity absorbents at 1740 cm-1, a spectrum corresponding to v(C = O) group vibration, were shifted by a combination of organic carbon chain graphene. The explanation for the spectrum of PDMS/graphene detection signals is assigned at 1257 cm^{-1} and 1099 cm-1 inclusive Si-C stretching vibration. The other reason for forming the matrix polymer or composites matrix is that no spectra appear. Functionalized graphene is not found around 790 and 950 cm-1, which means coordination bonds related to Si-OH groups.

On the other hand, structural features of the copolymers were established by FT-IR spectroscopy. Figure 2 display the FT-IR spectra of the copolymers as an example. There is no obvious variance of intensity, and the band absorption positions are found between the block copolymers and are randomly segmented.

Raman Spectroscopy.

We used Raman spectroscopy as another confirmation technique besides IR. It is a nondestructive technique that gives related structural information on carbon-skeleton materials or polymers. Raman spectroscopy of PDMS-graphene composite shown in Fig. 4 was carried out using a laser (wavelength 532 nm). The carbon group for the PDMS-peak wavelength spectrum is situated between 1300–1400 cm-1 and peaks slightly around 1550-1615cm-1 for characteristic peaks of graphene nanopowder. There is a proportional relationship between the intensity of graphene and PDMS polymer carbon structures. The increasing intensity with more graphene inside the polymer matrix demonstrated the well-dispersed and uniform distribution of graphene in a PDMS polymer cross-section. Also, there are considerable and progressive changes of intensity and widening of PDMS characteristic peaks before and after mixing with nanopowder graphene, confirmed with TEM analysis, shown in Figs. 7–9.

Figure 5 displays the spectrum intensity for nanoparticles (Ag and Cu) on the surface of PEI (polyethyleneimine) with spread speak appearing for PEI structure, especially for the (NH) amines group—confirming the assembly of nanoparticles on the PEI polymer. We also used UV spectrum analysis for a more detailed understanding.

To be more accurate, we use another optical characteristic for the prepared composite polymer. UV spectroscopic has been conducted to measure both direct and diffused light. Figure 7 shows that various spectrum absorbents at different wavelengths are a concept of Lambert's law. By comparing three spectra of absorbance PDMS/graphene, NPs/PEI, and copolymers, we found the absorbent properties

change intensity. There is significant evidence that the nanoparticles Ag, Cu, and nanographene filled the transmitted space (gaps), and the recorded height transmitted and disappears in other peaks in our structure.

SEM Characteristics

Scanning electron microscopy (SEM) SURFACE morphology was conducted using field emission Scanning Electron Microscopy involving a Quanta TM 3D FEG (FEI Company, USA) apparatus. All SEM images were created by an Everhart Thornley Detector (ETD) designed at a voltage of 5e30 kV.

A scanning electron microscope (SEM) has been used to characterize the morphological surface features' cross-section of each PDMS and PEI, SEM. Figure 6 shows that both of the polymers' surfaces are smooth without any cracking or deformation compared to Figs. 6a and 6b, which shows many cracks on the surface of different composite polymers varnished with graphene nanotubes and numerous nanoparticle conductive metals. Figure 6(b) displays a graphene/PDMS composite matrix with some defection and bending deformation on the composite composition. It is a good indicator that the new composite will be extremely flexible and wearable due to the PDMS' nature and because it is well stamped with graphene in the PDMS form. In the original PDMS, the SEM images are tidy and unruffled (without gaps or empty filler). One advantage of PDMS is that it might be subject to an electrostatic charge or polarity between the sio2 group and different nanoparticles when arranged in different shapes, as shown in Fig. 6b.

On the other hand, when the same description is applied to the PEI polymer before grafting nanoparticles, SEM image 6a shows that the SEM surface is smooth without any fractures or faults. Figures 6a and 6b show the SEM micrographs of the cross-section typically look like the previously prepared composites recorded before the literature review. There is an uncommonly uniform dispersal of graphene in some parts of the figure. Overall, this confirms that there is good compatibility dispersion between the two phases of the mixture.

TEM Characterization.

All analyses were carried out by transmission Electron Microscope model H-9500 operated at 100–300 kV TEM accelerated electron gun Panorama LaB6, with a high diffraction pattern. Specimens were divided into single crystal silicon (Si) and quickened at a voltage range between 40Kv to 100Kv. A high-resolution camera with a diffraction length of 0.5m and a magnification between 18× and 450,000× was used with the resolution (objective lens) set to 0.5nm/5.0å (point), 0.34nm/3.4å (line).

Composite PDMS /Graphene.

The images display excellent dispersal and the coalition of nanographene in a long unfilled space of PDMS polymer. There is a big change between Figs. 7a and 7b, which confirms our explanation. Furthermore, the change confirms that despite the existence of the PDMS component and good distribution of graphene inside the PDMS matrix, it will prevent agglomeration or sedimentation during

the process, which leads to uneven physical properties of the composites. The TEM image indicates that the graphene nanostructure's walls are heterogeneous, rough, and spotted with extra materials compared to pure PDMS, as shown in Fig. 7a. We considered that some of the aggregation or deposition of graphene on the surface area of PDMS is rough in some parts and uniform in other parts of PDMS due to the preparation methods (density or concentration overview).

Graphene and (Ag, Cu) NPs assembled on PEI.

Figures 8a and 8b show that TEM contrast in PEI/NPs polymer is accomplished via silver particles assembled on the surface of PEI due to the Ag reflection energy atom. This makes it easier to create bonds between amines groups and sliver atoms by gaining or losing electrons between two species. The size of Ag and Cu, around 10- 25 nm, causes filling in the PEI matrix cross-section. Furthermore, the homogeneity of PEI makes it easy to suspend fine nanoparticles in the solution. Also, Figure 8b indicates grafting nanoparticles (silver and copper) inside PEI polymer. It could be reforming new bonds between a pair of electrons on N-atoms and metal atoms of silver and copper particles through a metallic bond or galvanic bridge Cu / Cu + // Ag - / Ag. Regarding Figure 8a. we noticed Ag and CCu's distribution.

Composites PDMS-g-PEI

TEM characterization is used to investigate and estimate the change of surface morphology of different prepared materials (Graphene-PDMS, PEI-NPs, and Copolymer PEI-g-PDMS). Figures 9a and 9b illustrate the composition and dispersion of nanographene in the filler space of PDMS compared to Fig. 6b, where it appears smooth without any flocculation or deposition. The surfaces show good dispersion of layered graphene into a homogeneous PDMS-urea copolymer solution of PDMS-g-PEI. A TEM image is shown in Fig. 9a. NPs and graphene particles were recorded by distributed platelet shape with lower dimension than expected due to the formation of new composites inside polymers. Graphene-Cu or graphene-Ag composites Or could be present because NPs spread on graphene surfaces, which prevents them from appearing in a large amount in Fig. 9b. Furthermore, the TEM image in Figs. 9a and 9b explains both polymers' dispersal mechanism—integrated to form one copolymer without any distortion or voids. We believed the nanoparticles (Ag, Cu, and graphene) were chosen because each one has a unique physical and chemical property for forming chelating or bonded reactions together or with polymers carbon skeleton. Perfect PDMS /composites matrices can be in effect processed via the solution preparation casting and curing.

Figures 9a and 9b show that the copolymer (PEI-g-PDMS) was formed with a highly diverse distribution of graphene, silver, and copper inside the matrix to form new composites copolymer, which is flexible, stretchable, and conductive.

Particle size analyzer

Zetasizer Nano S90 (Malvern) modal Nano S90 analyzer carried out a particle size analysis on the liquid phases. It is operated by Red laser (632.8nm, 4 mW) and used a Zetasizer instrument that works at a

receptor angle equal to 90 degrees to make it easy to investigate and estimate particles suspended inside the liquid phase located between 1nm to 5 microns in diameter. Moreover, it is considered an important tool to evaluate and understand our colloidal solution and charge its physical properties, rheology behaviors, capacity, and efficiency ions charge, depletion, deposition, or precipitated particles. Figure 10 shows that the silver and copper nanoparticles are spread uniformly and suspended over the whole polyethyleneimine phase, which is good evidence of a new matrix's complete miscibility without any deformation. Furthermore, new sites or bonds will form. In addition, with the average volume of the particles at 193 nm, it is easier to carry a charge.

Figure 10a shows that though the particle size is somewhat larger at 920 nm, it might be related to the electrostatic or inter-inter Vander Waals force between graphene depletion or its agglomeration a TEM of surface morphology confirmed it. This showed good dispersal in some areas and flocculated in PDMS-graphene. However, it could be caused by a chain of a double layer (ions charge) forming from outers layers of graphene walls, which makes tubes (resonance π-π bond). This will be the main reason for the augmentation of conductivity in the whole final composite copolymer.

An EDAX analysis was done for composite copolymer (PDMS-g-PEI) to illustrate the main composition of impregnated nanoparticles inside the copolymer skeleton structure. There are copper, silver, and carbon (graphene), confirmed by previous analysis recorded in Fig. 12. The ion coupled plasma (ICP) for a sample of PEI-NPs contains the same elemental silver and copper composition, thus providing good evidence of the copolymer preparation (PDMS-g-PEI).

3.2 Mechanicals characterization.

The self-healing process and the tensile test are important methods to investigate our co-part polymers composites' mechanical properties. Figure 13 shows large differences before and after a combination of copolymers (PEI-NPs and PDMS-graphene) form one block copolymer. In Fig. 12, two polymers are compared by increasing the tensile strain by 10% compared to the PDMS /graphene polymer. The results also expose that the self-healed composite copolymer's tensile strength regains up to 90% of its original value.

4. Conclusion

To conclude, the copolymers' unique characteristics—robustness, flexibility, and good conductivity depend on the type of assembled nanomaterials, physical behaviors, and the chemicals created by bonding or chelating. The field of assembling or grafting carbon nanomaterials to diversify their properties creates applications in various fields. We created a flexible antenna that is easily wearable and non-toxic. We recorded the effect of grafting or combining nanoparticles graphene and copper and silver as a sandwich. We completely changed a new composite (copolymer) with nanostructures, such as graphene-carbon nanoform structures, by an sp2 hybridization mechanism. Using organosilanes in addition to PEI (polyethyleneimine) to broaden carbon nanomaterial behaviors and properties is an important way should be overwork.

The stretchable and formable patch antenna focuses on the material sandwich used in fabrication, such as PDMS-graphene/PEI-NPs composites.

We have characterized, fabricated and investigated, its improvement in all physical properties. For instance, we carried out electrochemical characteristics like EIS, impedance measurement to estimate new composites' conductivity, and comparison between initial and final product. In some of the mechanical tests applied to the copolymer structure, we noticed the new copolymer (PDMS-g-PEI) has healing and tension strain. Furthermore, numerous experiments and analyses have been conducting to prove the composite's composition, surface morphology, and nanoparticles distribution. In this way, we created a flexible, wearable electronic device that can be used in the future.

References

1. J. S. Noh. Polymers, 2016 8(4) 123
2. J.Y. Woo, K.K. Kim, j.T.Kim Lee, C.S. Han, C.S. Nanotechnology,2014, 25(28) 285203
3. S. Zhang, Y. Li, Q. Tian, L. Liu, W. Yao.; P. C.Chi, Zeng, N.Zhang, N., W. Wu, Highly. J. Mater. Chem. C **6**(15), 3999–4006 (2018)
4. M.K.ShinJ.; Oh, M. Lima, M. Kozlov,. E.; Kim, S.J.; Baughman, R. H. Elastomeric Advanced Materials. John Wiley & Sons, Ltd June 25, 2010 pp 2663–2667
5. L. Cai, S. Zhang, J. Miao, Z. Yu, C. Wang, ACS Nano (2016) 10 (12), 11459–11468
6. K.S. Kim, Y. Zhao, H. Jang, S. Lee, Y.; Kim, J.M.; Kim, K.S.; Ahn, J.H.; Kim, P.; Choi, J.Y.; Hong, B. H. Nature **457**(7230), 706–710 (2009)
7. S. Stankovich, D.; Dikin, G.H.B. Dommett, K.M. Kohlhaas, E.J. Zimney, E.A. Stach, R.D. Piner, S.B.T. Nguyen, R.S. Ruoff, Nature,2006 442 (7100)
8. C.Yan,J. Wang, W. Kang, M. Cui, X. Wang, C. Foo, K.J. Chee, P.S. Lee, Adv. Mater. **26**(13), 2022–2027 (2014)
9. M.Chen,L. Zhang, S. Duan, S. JingJiang, C. Li, Adv. Funct. Mater. **24**(47), 7548–7556 (2014)
10. F. Yakuphanoglu, B.F. Şenkal,.. J. Phys. Chem. C **111**(4), 1840–1846 (2007)
11. Y.FuA. Manthiram,.Chem. Mater. 2012 24 (15), 3081–3087
12. D. Borah, M.T. Shaw, S. Rasappa, R.A. Farrell, C. O'Mahony, C.M. Faulkner, M. Bosea, P. Gleeson, J.D. Holmes, M.A. Morris, Appl. Phys. Rev **44**, 17 (2011)
13. J.D. C.AArnold, Y.P. Summers, R.H. Chen, D.Chen Bott, Polymer; Elsevier, 1989, Vol. 30, pp 986–995
14. C.M. Mahoney, J.A. Gardella, J.C. Rosenfeld,,Macromolecules 2002 35 (13), 5256–5266
15. C. E.Hamciuc, Hamciuc, & Cazacu,,Rev Roum Chim **54**, 1007–1013.56–16 (2009)
16. J.E. McGrath, D.L. Dunson, S.J. Mecham, J.L. Hedrick In Progress in Polyimide Chemistry I 1999 (pp. 61–105). Springer, Berlin, Heidelberg
17. M., Freebody,. (ed.). 2011. Photonics Spectra, 45(5), 45–47

18. D. Borah, M.T. Shaw, S. Rasappa, R.A. Farrell, C. O'Mahony, C.M. Faulkner, M. Bosea, P. Gleeson, J.D. Holmes, M.A. Morris, "Appl. Phys. Rev **44**, 17 (2011)
19. C.A. MacK, Fifty Years of Moore's Law. IEEE Trans. Semicond. Manuf. **24**, 202–207 (2011)
20. J.M. Raquez, Y. Habibi, M. Murariu, P. Dubois, Polylactide (PLA)-Based Nanocomposites. Progress in Polymer Science. Elsevier Ltd October 1, 2013, pp 1504–1542
21. A.Vaglio Pret, P. Poliakov, R. Gronheid, P. Blomme, M. Miranda Corbalan, W. Dehaene, D. Verkest, J. Van Houdt,D. Microelectronic Engineering; Elsevier, 2012; Vol. 98, pp 24–28..(2012)04.013
22. I.S. A.Biswas, A.S. Bayer, T. Biris, E. Wang, F. Dervishi, Faupel, Elsevier J **15**, 2–27 (2012)
23. S.B. Darling, Directing the Self-Assembly of Block Copolymers. Progress in Polymer Science (Oxford). Pergamon October 1,2007 pp 1152–1204
24. W.T. H.WLi, Huck,. Nano Lett.2004 4 (9), 1633–1636
25. J.K. I.Bita, S.J. Yang, C.A. Yeon, E.L. Ross, Thomas, K.K. Berggren, Science **(80-**(5891), 939–943 (2008) 321)
26. T. Ghoshal, R. Senthamaraikannan, M.T. Shaw, J.D. Holmes, M.A. Morris, M. A. In Situ Hard Mask Materials: Nanoscale,2012,4 (24), 7743–7750
27. M. T.Hirai, C.C. Leolukman, E. Liu, Y.J. Han, T. Kim, YIshida, M.A. Hayakawa, Kakimoto, Adv. Mater. **21**(43), 4334–4338 (2009)
28. P.Lee,J. Lee, H. Lee, J. Yeo, S. Hong, K.H.; Nam, D. Lee,. Adv. Mater.2012,24 (25), 3326–3332
29. F. Xu, Y. Zhu, Adv. Mater. **24**(37), 5117–5122 (2012)
30. G.F. W.Gaynor, M.D. Burkhard, P. McGehee, Peumans, Adv. Mater **23**(26), 2905–2910 (2011)
31. C.A. Arnold, J.D. Summers, Y.P. Chen, R.H. Bott, D. Chen, J.E. McGrath Structure-Property Behaviour of Soluble Polyimide-Polydimethylsiloxane Segmented Copolymers. In Polymer; Elsevier, (1989) 30, pp 986–995
32. C.M. Mahoney, J.A. Gardella, J.C. Rosenfeld, Macromolecules 2002, 35 (13), 5256–5266
33. E. Hamciuc, C., Hamciuc, & Cazacu, Rev Roum Chim **54**, 1007–1013 (2009)
34. J.E. McGrath, D. Dunson, S.J. Mecham, J.L. Hedrick, Adv. Polym. Sci. **140**, 62–105 (1999)
35. X.Pei, G.Chen, X., Fang, High Perform. Polym. **23**(8), 625–632 (2011)
36. M.Krea,.D.N. Roizard, Moulai-Mostefa, D.Sacco,. J. Memb. Sci 2004 241 (1), 55–64
37. C.J. Wohl, B.M. Atkins, M.A. High Perform, Polym. **24**(1), 40–49 (2012)
38. J.E. I.Yilgör, McGrath,. Springer-Verlag, 2005 pp 1–86
39. W.C. Liaw, J. Chang-Chien, H. Kang, Y.L.; Cheng, L.; Fu, L. W. A. Polym. J. 2008 40 (2), 116–125
40. A.J. A.Mata, S. Fleischman. Roy, S. Microdevices **7**(4), 281–293 (2005)
41. R.H. Baughman, A.A. Zakhidov, Heer Science August **2**, 787–792 (2002) W.A De
42. S.H. Lee, D. Lee, H.; Lee, W.J.; Kim, S. O. Adv. Funct. Mater. **21**(8), 1338–1354 (2011)
43. J.M. Schnorr, T.M. Swager, Chemistry of Materials. American Chemical Society February **8**, 646–657 (2011)

44. J.N. Coleman, U. Khan, W.J. Blau, Y.K; Gun'ko.. Carbon. 2006, pp 1624–1652
45. M.H. Al-Saleh, U. Sundararaj,.Carbon N. Y. **47**(7), 1738–1746 (2009)
46. E. Frackowiak, V. Khomenko, K. Jurewicz, K. Lota, KF Béguin,.In Journal of Power Sources; Elsevier,2006,153, pp 413–418
47. J. Li, X. Cheng, J. Sun, C. Brand, A.; Shashurin, M. Reeves, M.J. Keidar, Appl. Phys. **115**(16), 164301 (2014)
48. J. J.Hwang, K. Jang, K. Hong, K.N. Kim, J.H. Han, K. Shin, C.E. Park, Carbon N. Y. **49**(1), 106–110 (2011)
49. P.P.ötschke,K.Kobashi,T.; Villmow, T. Andres, M.C.; Paiva, J.A. Covas,. Compos. Sci. Technol. 201171 (12), 1451–1460
50. M. Yu, Q. He, Q.D. Yu, X. Zhang, A.; Ji, H. Zhang, C.; Guo, Appl. Phys. Lett. **101**(16), 163701 (2012)
51. S.K. Yadav, I.J.; Kim, H.I.; Kim, J.; Kim, S.M. HongC.M, Koo,. J. Mater. Chem. C **1**(35), 5463–5470 (2013)
52. S. Kazaoui, N. Minami, B. Nalini, Y. Kim, K. Hara, J. Appl. Phys 2005 98 (8), 084314
53. M.L. G.Mao, D.L.PriceY.S. Saboungi, H.F. Badyal, Europhysics Lett. 2001 54 (3), 347
54. K.S. D.Kim, Yun, Patterning of Carbon Nanotube Films on P.D.M.S. Springer, 2013 Vol. 19, pp 743–748
55. Y. J.Chih, Chen,.; University of Waterloo, (2002)
56. A.V. J.Kurdi, Polymer, (Guildf) **44**(16), 4533–4540 (2003)
57. J. J.Ren, M. Zhou, Sep. Purif. Technol. **74**(1), 119–129 (2010)
58. J.N. Coleman, M. Cadek, M.K.P. Ryan, A. Fonseca, J.B. Nagy, Polymer **47**(26), 8556–8561 (2006)
59. J.M. Raquez, Y. Habibi, M. Murariu, P. Dubois, P Progress in Polymer Science. Elsevier Ltd October **1**, 1504–1542 (2013)
60. M.A. S.Saeidlou, H. Huneault, C.B. Li, Park, J. Appl. Polym. Sci. 2014 131 (22)
61. E.LogakisC. Pandis, V. Peoglos, P. Pissis, C. Stergiou, J.; Pionteck, J. Polym. Sci. Part B Polym. Phys **47**(8), 764–774 (2009)
62. E. Logakis, C. Pandis, V. Peoglos, P. Pissis, C. J. Polym. Sci. Part B Polym. Phys. 2009 47 (8), 764–774
63. M.L. M.Trujillo, A.J. Arnal, A. MüllerM, Mujica,.; Polymer (Guildf). 2012 53 (3), 832–841
64. J.F. Vega, J. Fernández-Alcázar, J.V. López, R.M. Michell,.; R.A. Pérez-Camargo, B. Ruelle, J. Martínez-Salazar, M.L. Arnal, P. Dubois, A.J. Müller, J. Polym. Sci. Part B Polym. Phys. 2017 55 (17), 1310–1325
65. M. Moniruzzaman, K.I. Winey, American Chemical Society 2006, pp 5194–5205
66. J.N. Coleman, U. Khan, W.J. Blau, Y.K.; Gun'ko,.. Carbon. 2006 pp 1624–1652
67. M. Hegde, U. Lafont, B. Norder, E.T. Samulski, M. Rubinstein, T. J Polymer (Guildf) **55**(16), 3746–3757 (2014)

68. P. Klonos, Z. Terzopoulou, S. Koutsoumpis, S. Zidropoulos et al., Eur. Polym. J. **82**, 16–34 (2016)
69. M. L.Bokobza, C. Rahmani, J.L. Belin, N.E. Bruneel, El, Bounia,.. J. Polym. Sci. Part B Polym. Phys. 2008 46 (18), 1939–1951
70. L. Li, L.B. Li, M.A.; Hood, C.Y. Li, Polymer. Elsevier BV **9**, 953–965 (2009)
71. M. A.Beigbeder, M. Linares, P. Devalckenaere, M. Degée, D. Claes, Adv. Mater **20**(5), 1003–1007 (2008)
72. C.Y. C.Dewaghe, M. Lew, S.A. Claes, P.Dubois Belgium,. In Polymer-Carbon Nanotube Composites: Preparation, Properties and Applications; Elsevier Ltd, 2011 pp 718–745
73. K.T.S. Kong, M.; Mariatti, A.A. Rashid, J.J.C Compos. Part B Eng **58**, 457–462 (2014)
74. T. D.Hu, K. Cheng, R. Xie, Sensors 2015 15 (10)
75. H.F. Zhang, M.K. Teo, C. Yang, C.. Mater. Sci. Technol. **31**(14), 1745–1748 (2015)
76. M. Nishio, M.Hirota,Y. Nature, and Consequences; Wiley,9 1998
77. O. Heaviside. Electromagnetic theory. Cosimo, Inc., 2008
78. G.T. R.Buchner, P.M. HefterP.M May, J. Phys. Chem. A **103**(1), 8–9 (1999)
79. B.E. Mellander, I. Phys. Rev. B **26**(10), 5886–5896 (1982)
80. G. Mao, M.L. Saboungi, D.L. Price,, Y. S.; Europhysics Lett **54**(3), 347 (2001)
81. C.H. Chan, H.W. Kammer Ionics, (Kiel) **23**(9), 2327–2337 (2017)
82. C.H. Chan, H.W. Kammer, Ionics (Kiel). 201521 (4), 927–934
83. C.H. Chan, H.W. Kammer, Ionics **22**(9), 1659–1667 (2016)
84. C.H.W. HChan In Pure and Applied Chemistry; De Gruyter, 2018, 90, pp 939–953
85. C.H.ChanH.W.; Kammer, L.H. Sim, S.N.Yusoff,A.Hashifudin Winie, T. Ionics, (Kiel) **20**(2), 189–199 (2014)
86. M.Chen,L. Zhang, S. Duan, S. Jing, H. Jiang, C. Li, Adv. Funct. Mater. **24**(47), 7548–7556 (2014)

Figures

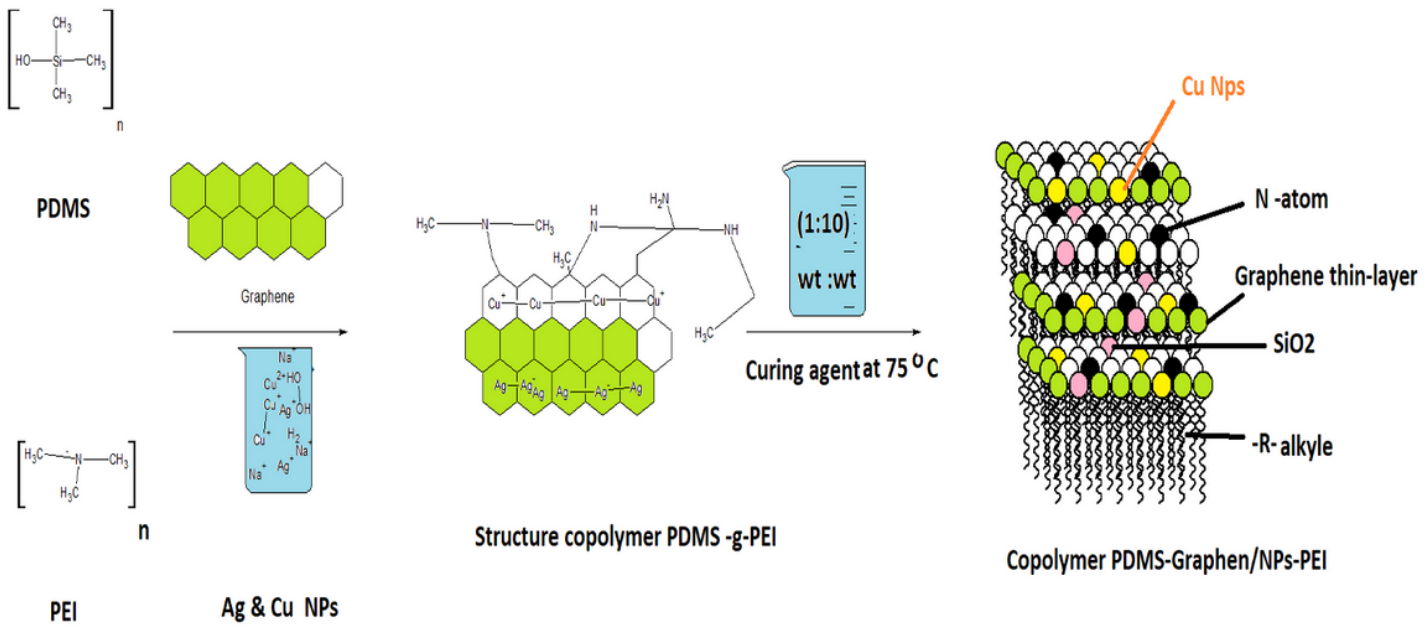

Figure 1

Pathway of copolymer PDMS –G/NPs- PEI preparation.

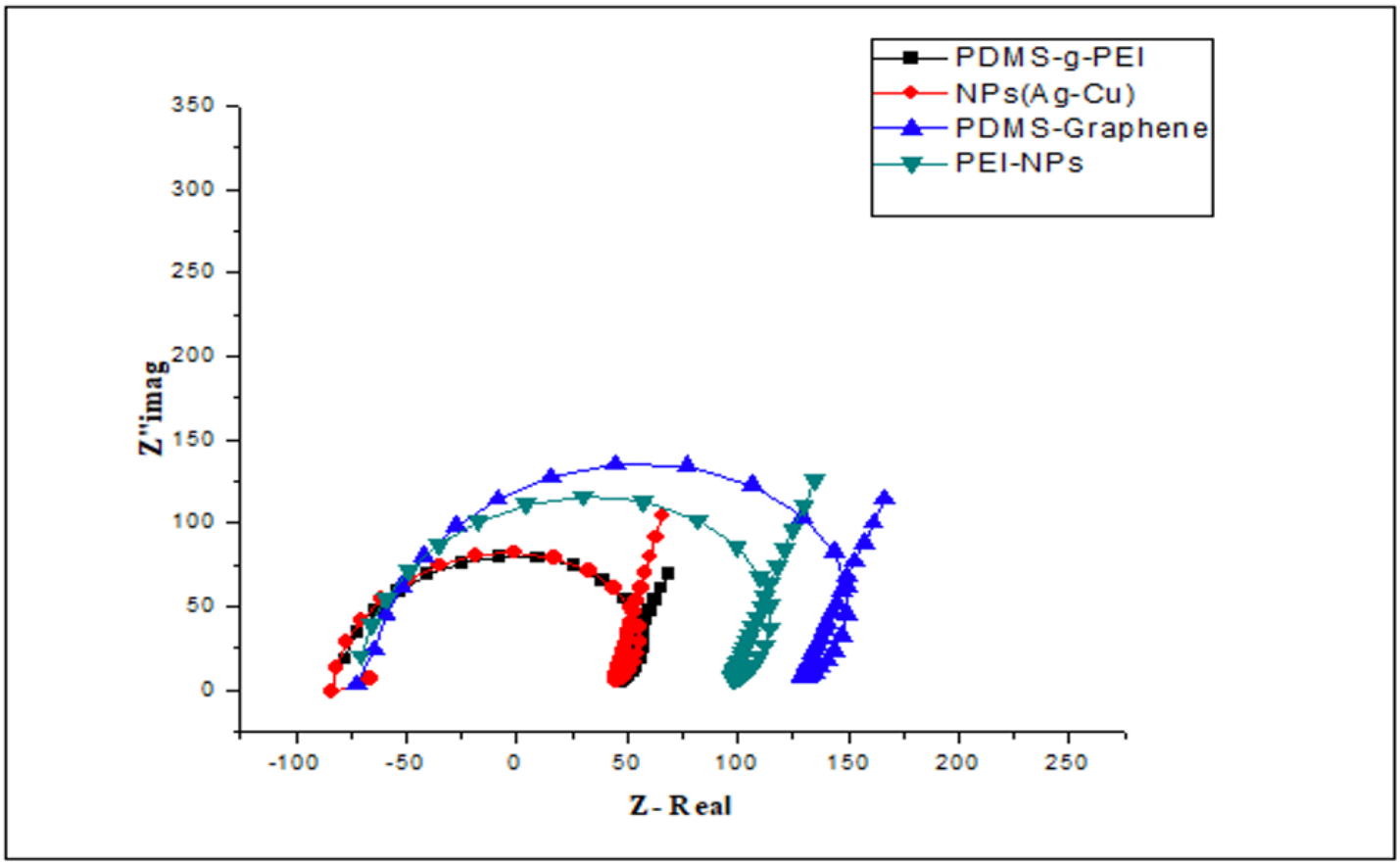

Figure 2

The impedance of different prepared solutions used to copolymer composition.

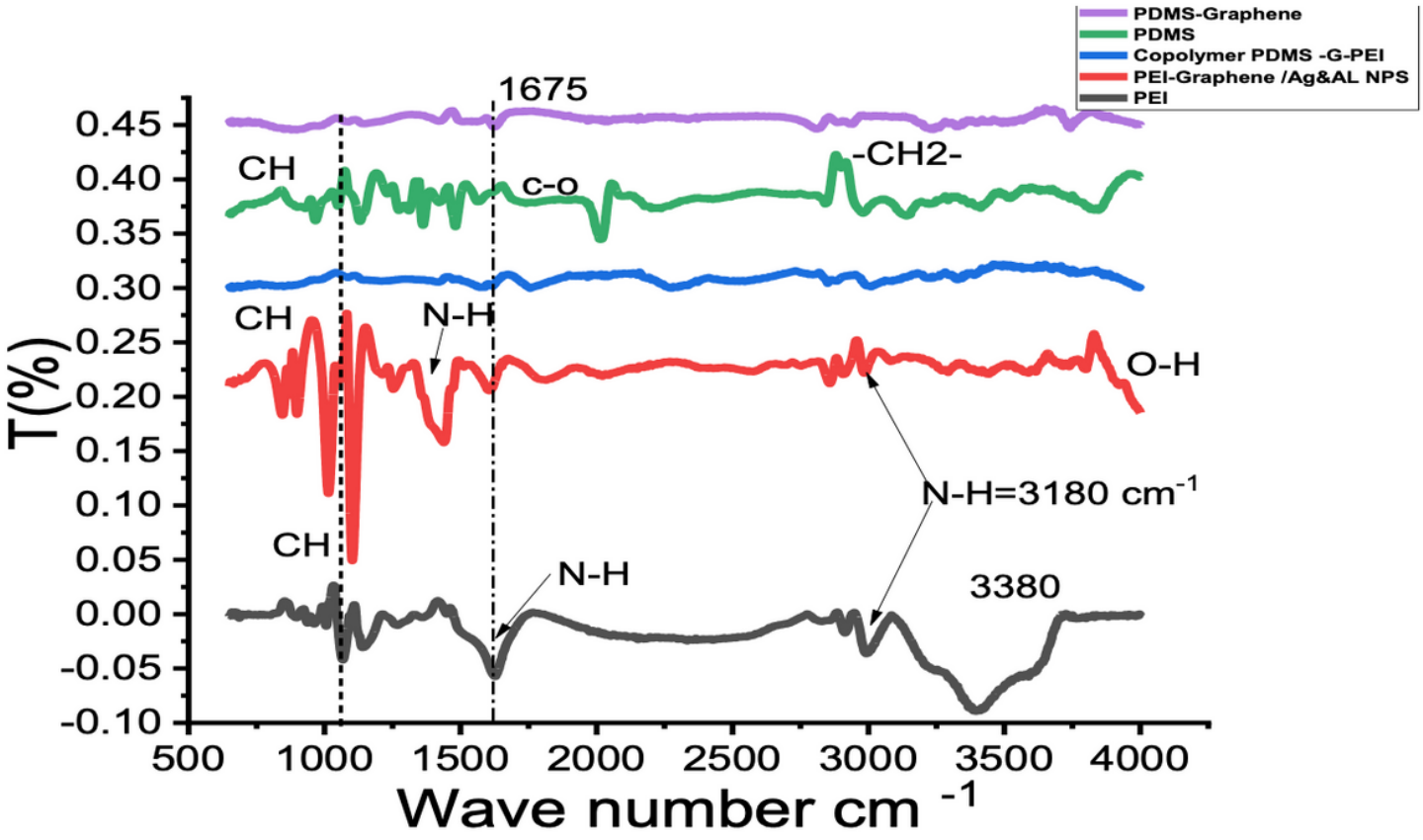

Figure 3

IR spectrum characterization

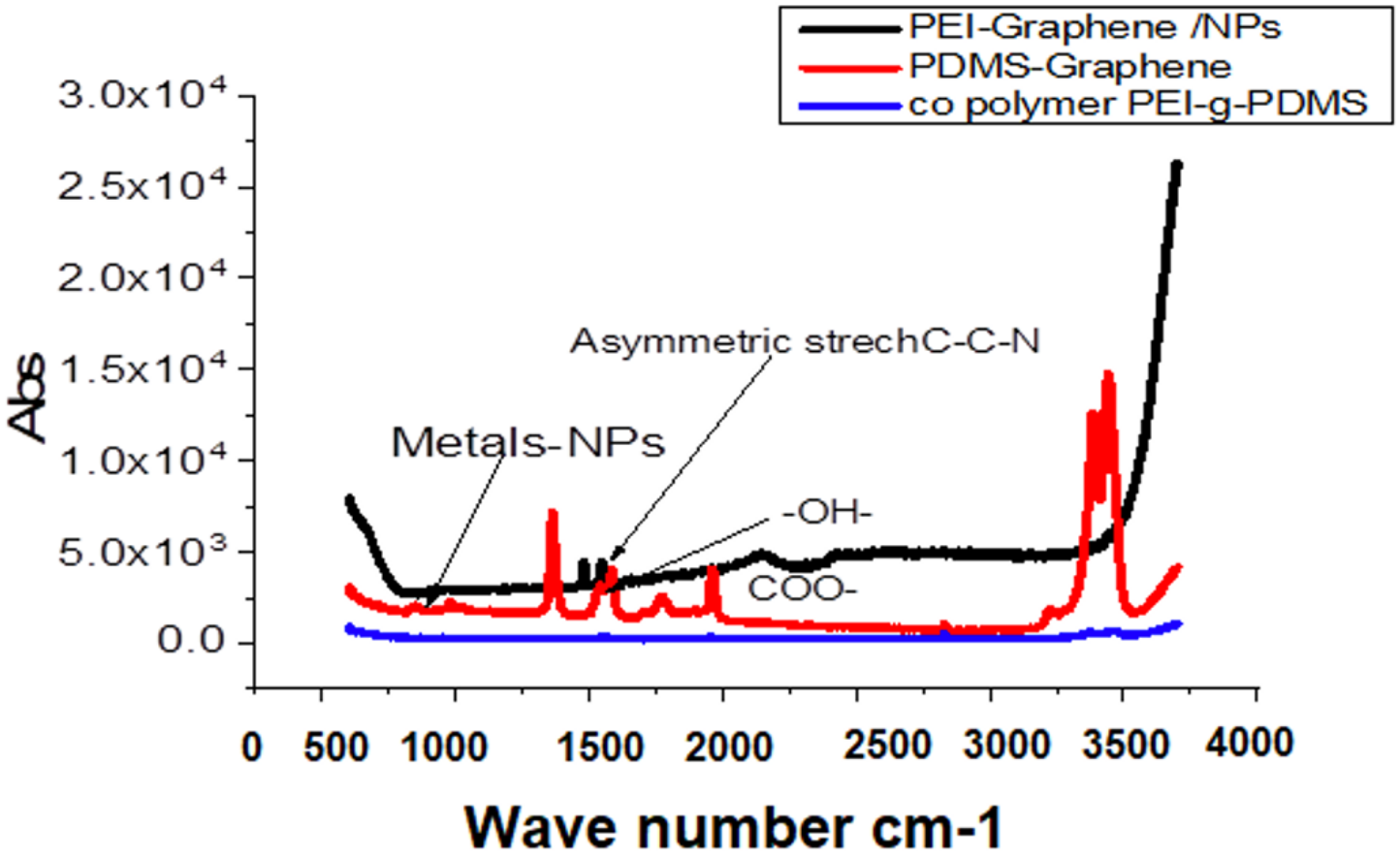

Figure 4

Raman analysis for different composites.

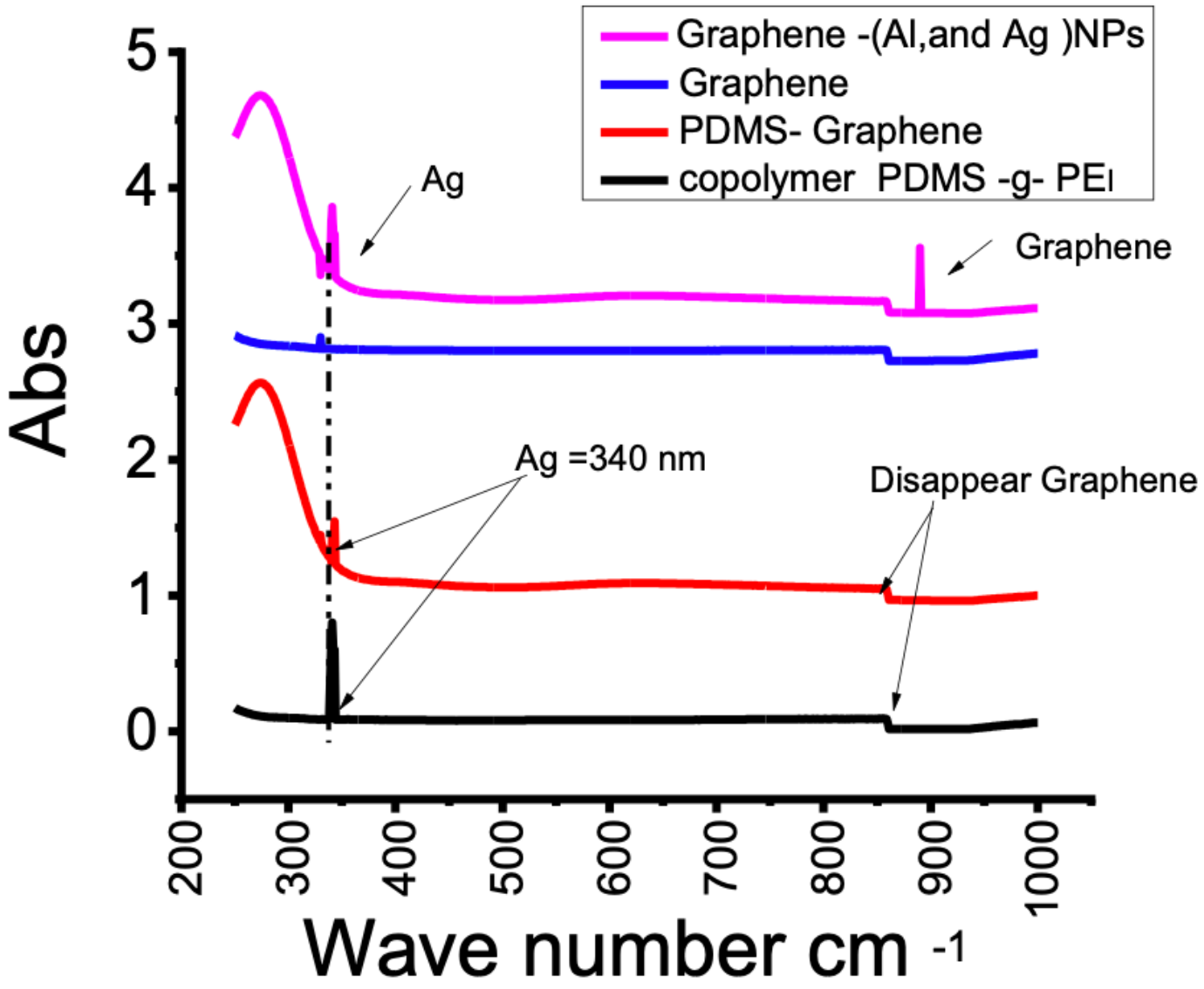

Figure 5

UV for composites structure

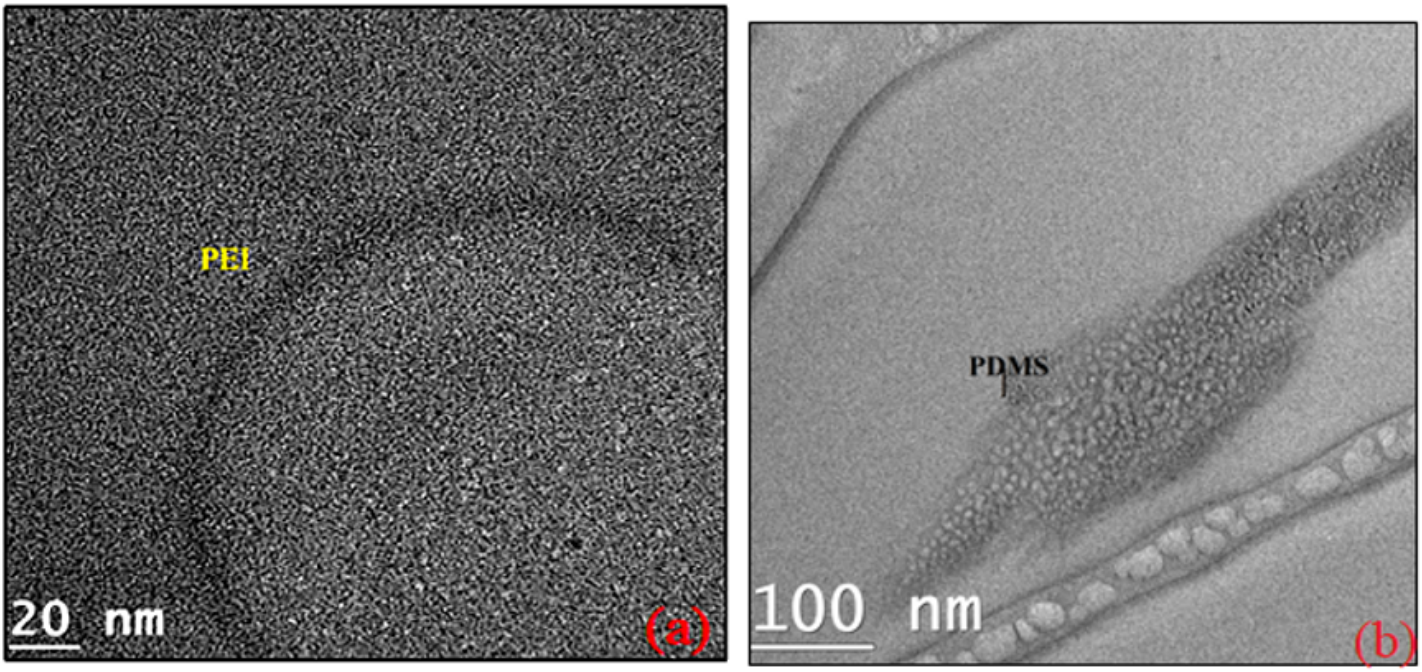

Figure 6

SEM for a) PEI b) PDMS

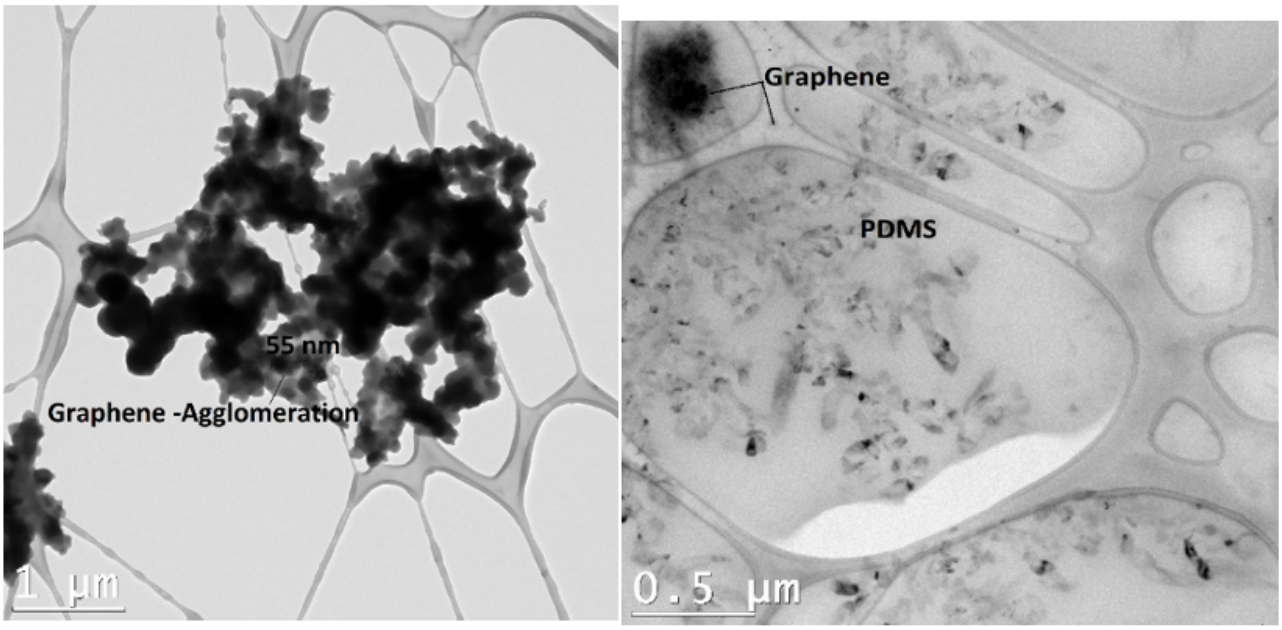

Figure 7

TEM a) Graphene b) PDMS /Graphene solution

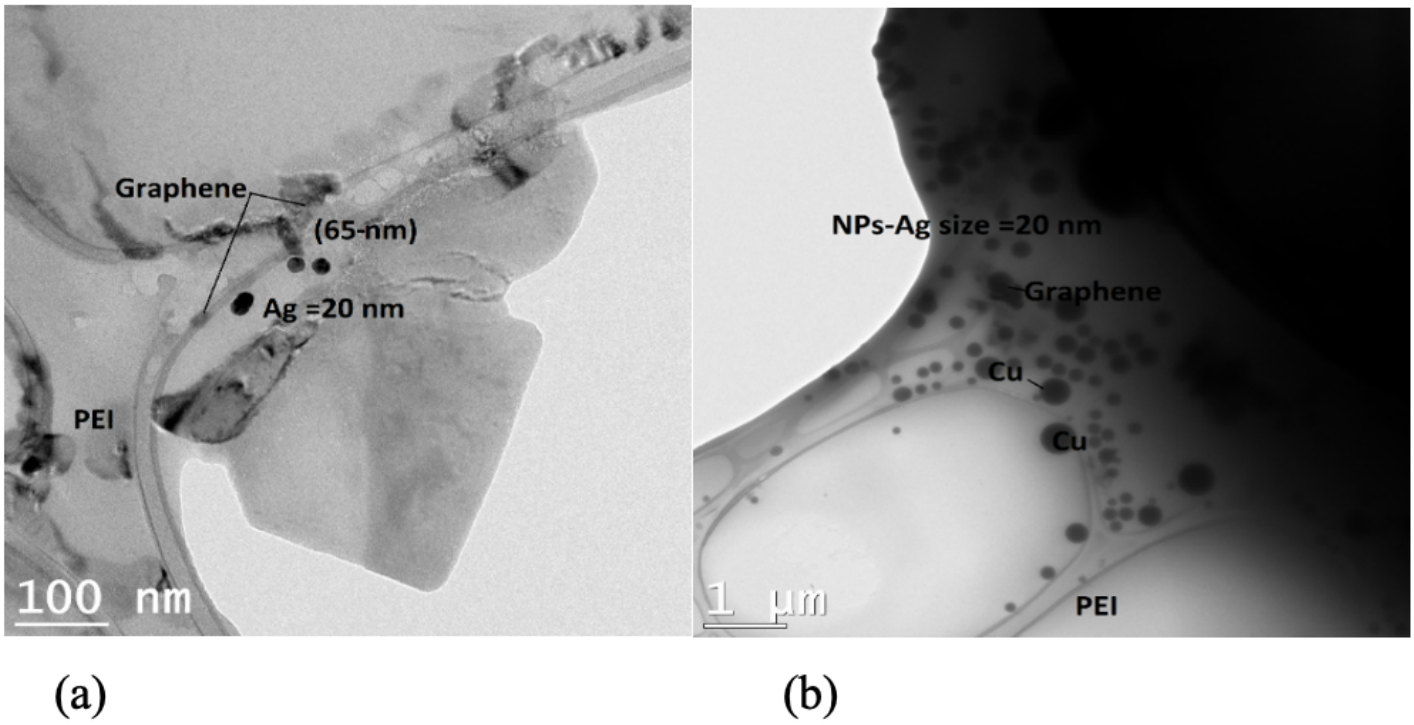

Figure 8

TEM a) PEI –Graphene b) PEI-Graphene/NPs assembled

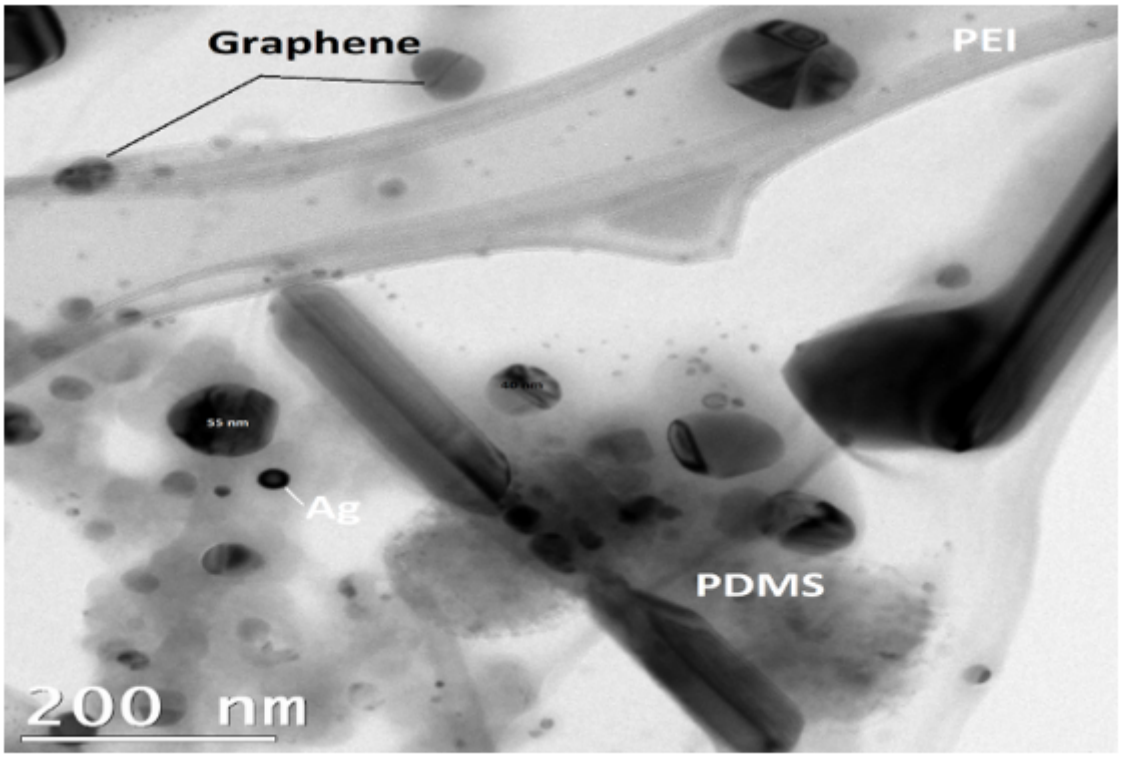

Figure 9

TEM PDMS –Graphene /NPS –PEI Co-polymer composites.

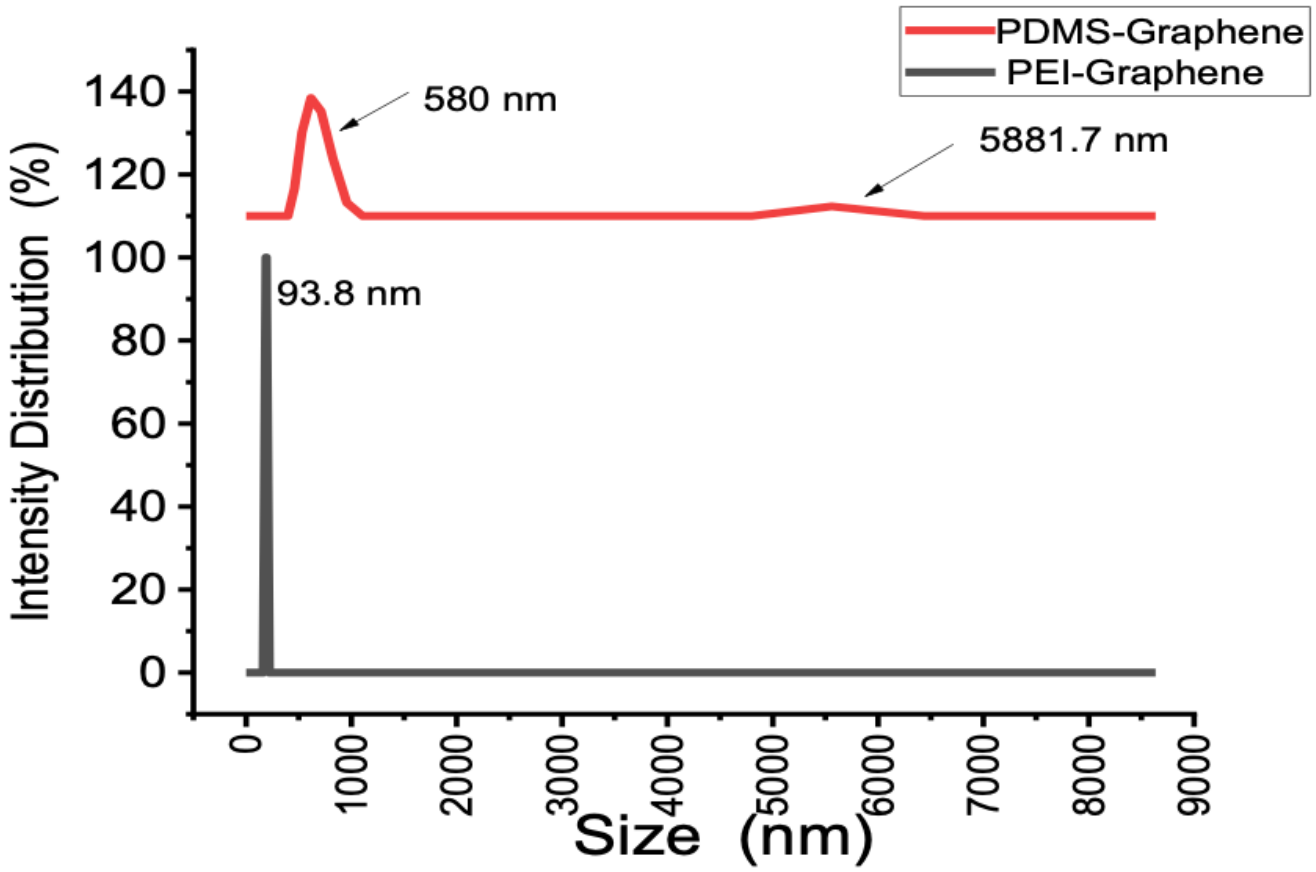

Figure 10

Particle size Analyzer a) PDMS /graphene b), PEI polymer assembled nanoparticles and graphene.

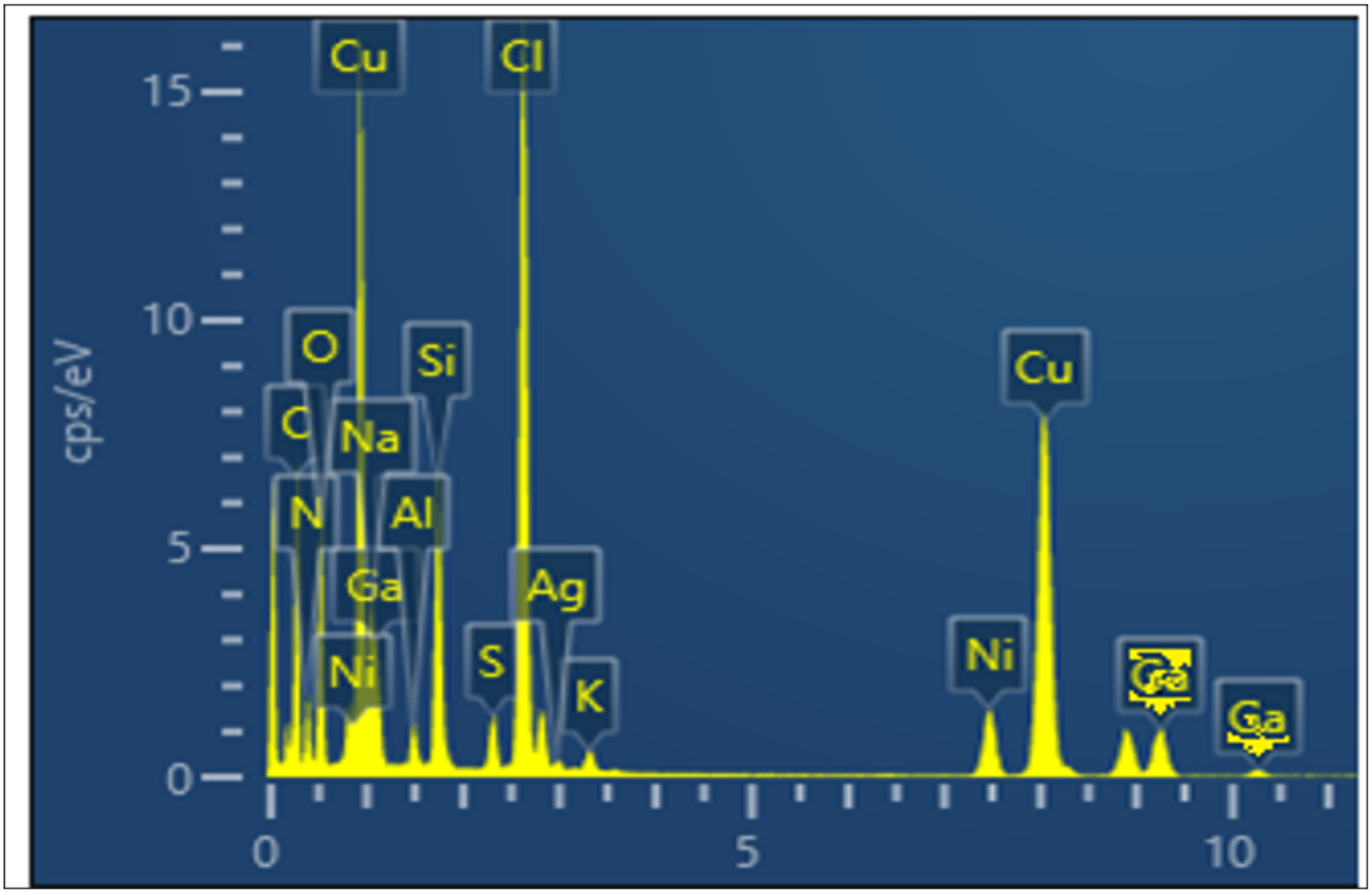

Figure 11

EDAX characterization of copolymers.

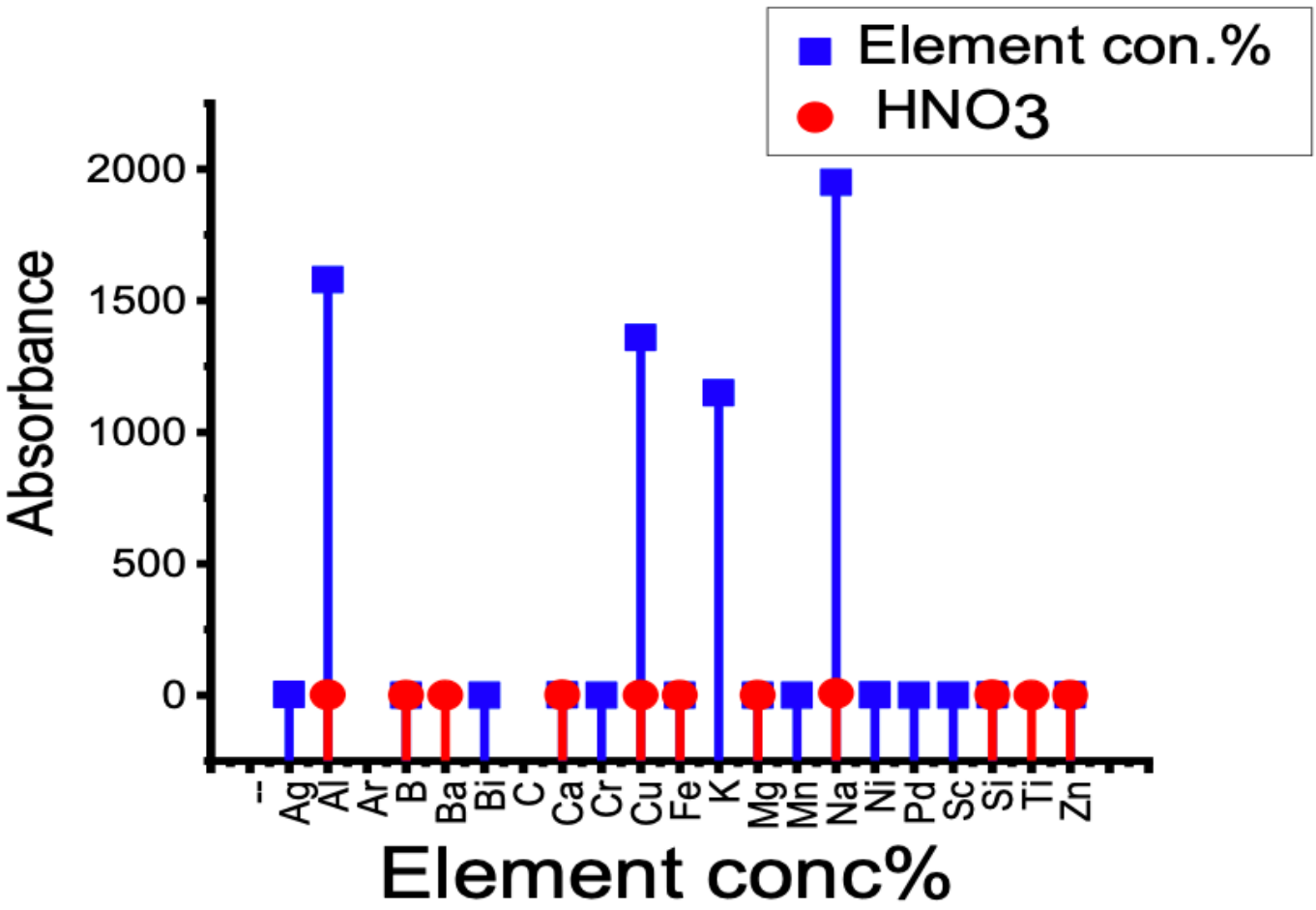

Figure 12

ICP analysis PEI-NPs.

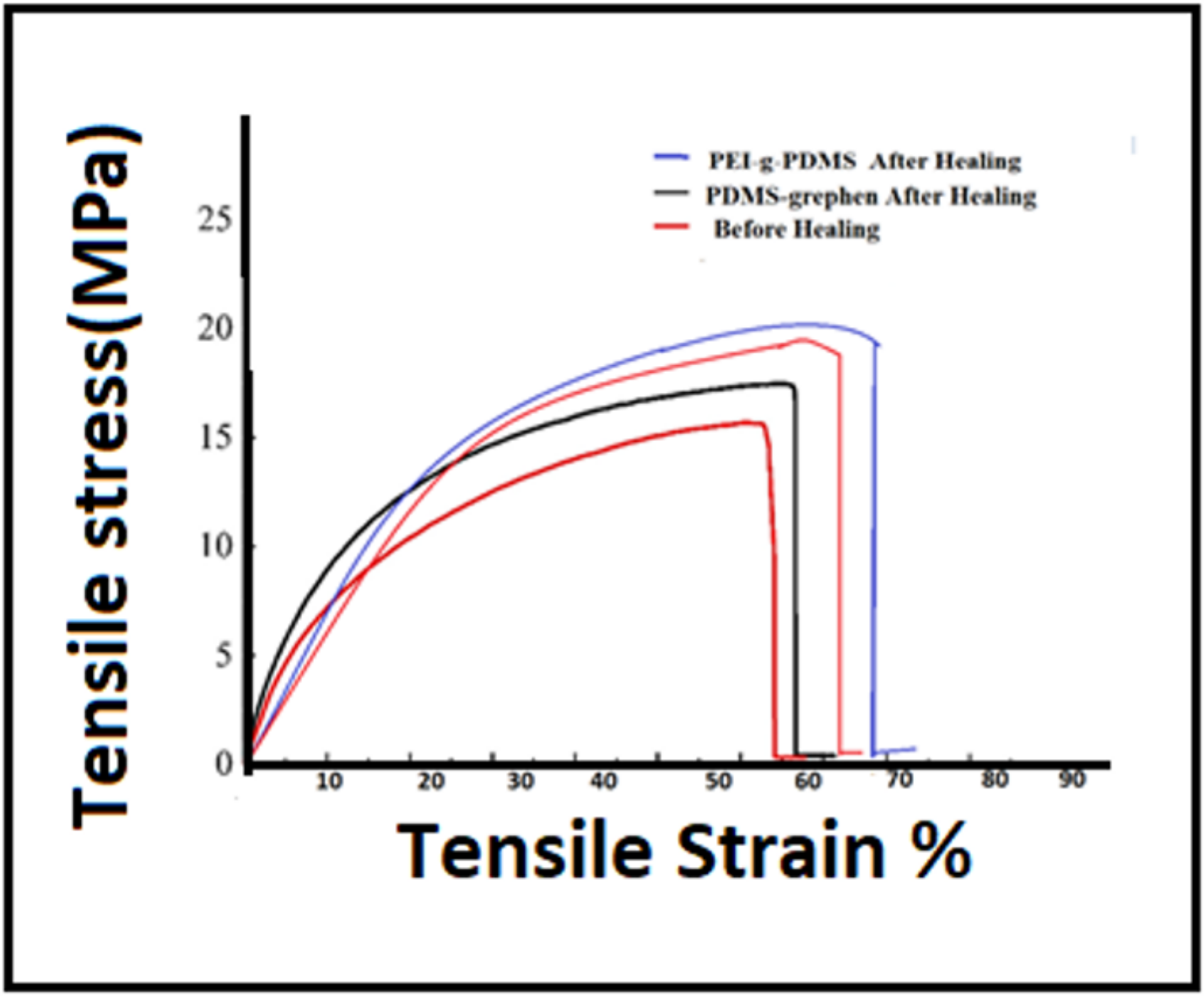

Figure 13

Stress-strain of free-standing PDMS, and co-polymers PDMS-graphene-PEI before and after the self-healing process.